Supporting Information

Dynamic and Reversible Fluorescence Imaging of Superoxide Anion Fluctuations in Live Cells and in Vivo

Wen Zhang[†], Ping Li[†], Fan Yang, Xiufen Hu, Chuanzhi Sun, Wei Zhang, Dezhan Chen, Bo Tang[*]

College of Chemistry, Chemical Engineering and Materials Science, Engineering Research Center of Pesticide and Medicine Intermediate Clean Production, Ministry of Education, Key Laboratory of Molecular and Nano Probes, Ministry of Education, Shandong Normal University, Jinan 250014, P.R. China. Shandong Normal University, Jinan 250014, P. R. China.

[*]E -mail: tangb@sdnu.edu.cn

Table of Contents

page

1. Computational study

To verify the effect of conversion from electron-donating hydroxyl to electron-withdrawing carbonyl, natural bond orbital (NBO)[1-4] analyses were performed at the B3LYP/6-31G(d, p) level to assign the atomic charges (Q) based on the optimized structures in Gaussian 03[5, 6] (Figure S1a). The calculated charges are listed in Figure S1b. According to the results, the charges on caffeic acid moiety of TCAO are decreased compared with TCA, from 0.133 to 0.112 (left caffeic acid) and 0.131 to 0.105 (right caffeic acid) respectively, indicating electrons transfer from tripolycyanamide to caffeic acid moiety by changing hydroxyl to carbonyl, which agree with our original intention.

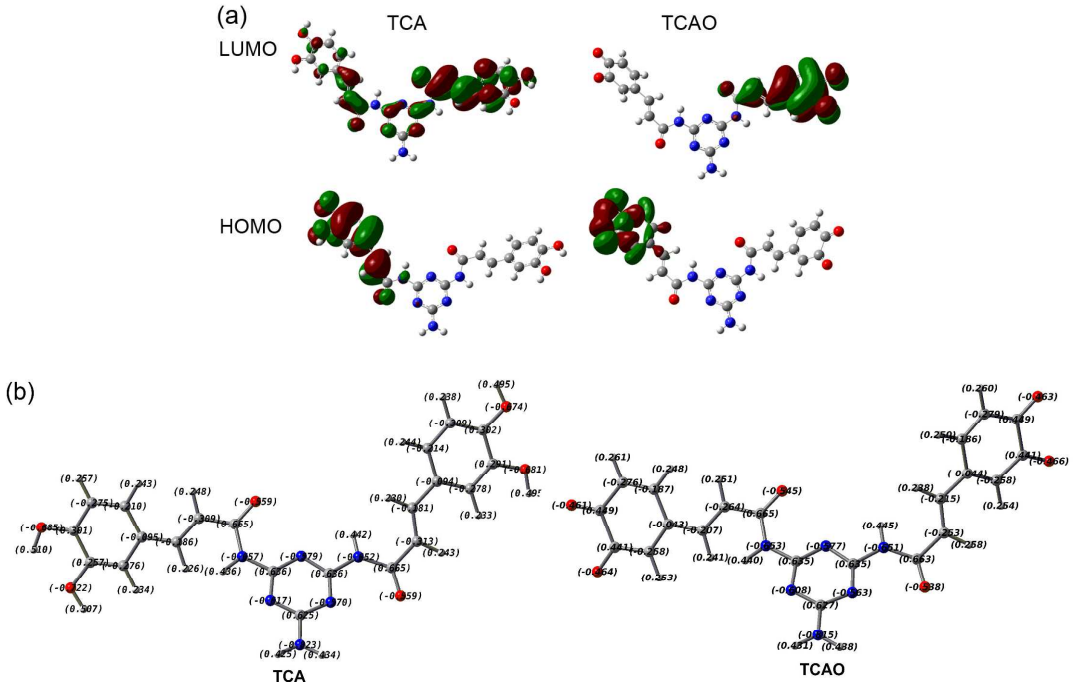

Figure S1 (a) The HOMO and LUMO orbitals of TCA and TCAO. (b) The calculated atomic charges of TCA and TCAO.

2. Materials and reagents

All chemicals were available commercially and the solvents were purified by conventional methods before use. Tripolycyanamide was purchased from Tianjin Kemiou Chemical Reagent Company and caffeic acid was from Adamas Reagent. Rotenone and malonic acid (MA) were purchased from Aladdin Industrial, Superoxide dismutases (SOD), Xanthine Oxidase, Xanthine and buthionine sulphoximine (BSO) from Sigma-Aldrich, Purinol from Guangdong PIDI Pharmaceutical Company, 2,3-Dimercaptopropanol (BAL) from TCI and Arcoxia from Merck & Co. Reactive oxygen species were

as follows. H_2O_2, tert-butylhydroperoxide (TBHP), and hypochlorite (NaOCl) were delivered from 30%, 70%, and 10% aqueous solutions respectively. Hydroxyl radical (•OH) was generated by reaction of 1 mM Fe^{2+} with 200 μM H_2O_2. Nitric oxide (NO) was used from stock solution prepared by sodium nitroprusside. Singlet oxygen ($^1O_2$) was prepared by the ClO^-/H_2O_2 system. Peroxynitrite was used from stock solution 10 mM in 0.3 M NaOH. Superoxide ($O_2^{\cdot-}$) was delivered from KO_2 in DMSO solution or from Xanthine Oxidase.

^{1}HNMR spectra were determined by 300 MHz and 600 MHz using Bruker NMR spectrometers. The mass spectra were obtained by Bruker maXis ultra-high resolution-TOF MS system. The melting points were measured by a SGW X-4 Melting Point Tester. The one-photon excited fluorescence spectra measurements were performed using FLS-920 Edinburgh fluorescence spectrometer. Two-photon excited fluorescence spectra were measured using a Tsunami 3941-M3-BB: Ti: sapphire femtosecond laser as exciting light source (800 nm) with a pulse width of <150 fs and a repetition rate of 80 MHz, and USB2000 (bought from Ocean Optics Inc.) was used as the recorder. Cell Extracts were prepared by BILON92-IIL ultrasonic disintegrator (Shanghai Bilon Materials Inc.).

3. Synthesis of probe TCA

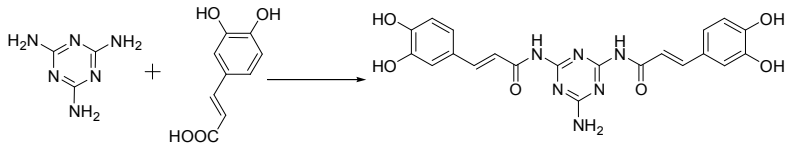

TCA

First, triethylamine (1.0 mL), 1-hydroxybenzotriazole (0.636 g, 3.0 mmol) and EDC (0.576 g, 3.0 mmol) were added to a solution with tripolycyanamide (0.126 g, 1.0 mmol) and caffeic acid (0.525 g, 3.0 mmol) in dinethylformamide (1.2 mL) and dichloromethane (8.0 mL). After the mixture was stirred over night at room temperature under nitrogen, it was concentrated in vacuum. The residue was purified by preparative thinlayer chromatography of silica gel GF_{254} with ethyl acetate/ hexamethylene (5:1) as eluent and light yellow product was obtained. mp: 240 °C; ^{1}H NMR (300 MHz, DMSO): δ 7.973 (m, 6H), δ 7.898 (d, 2H), δ 7.810 (d, 2H), δ 8.500 (s, 8H); ^{13}C HNMR (600 MHz, DMSO): δ 167.5, 143.2, 143.0, 129.5, 128.0, 125.9, 120.2, 118.1, 110.2, 109.3, 106.9; MS data, m/z: 451.4496 (M+H); IR: 1719 cm^{-1}.

The compound TCAO can be obtained by $O_2^{\cdot-}$ oxidation reaction. After adding excessive superoxide anion, dark yellow product was obtained. ^{1}H NMR (600 MHz, DMSO): δ 7.742 (m, 6H), δ 8.103 (d, 2H), δ 8.174 (d, 2H); ^{13}C HNMR (600 MHz, DMSO): δ 167.5, 162.3, 143.2, 143.1, 128.0, 125.7, 120.2, 110.2, 109.7; MS data, m/z: 447.3628 (M+H); IR: 1640 cm^{-1}.

4. $O_2^{\cdot-}$ titration experiment

The changes of TCA one-photon fluorescence spectra with $O_2^{\cdot-}$ of various concentrations were monitored. Good linear correlation was obtained. It indicated that TCA was able to qualitatively and quantitatively determine levels from KO_2 (Figure S2a). Besides, TCA also can monitor $O_2^{\cdot-}$ from Xanthine Oxidase (Figure S2b). Obviously, $O_2^{\cdot-}$ generated from KO_2 or enzymatic systems can trigger fluorescent enhancement of TCA consistently.

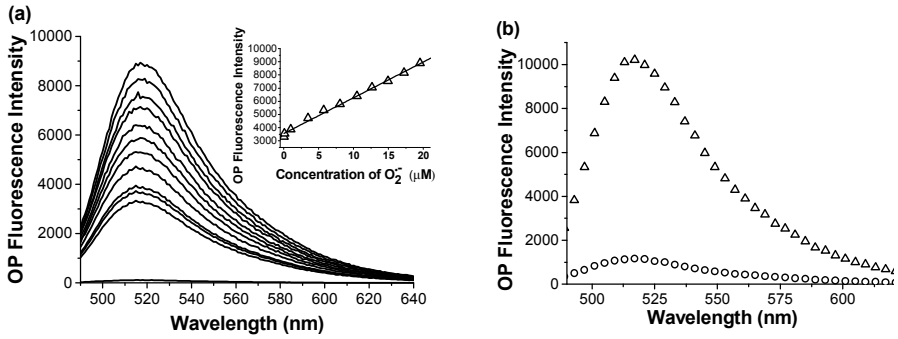

Figure S2 (a) One-photon fluorescence spectra of 10 μM TCA after adding various concentrations of $O_2^{\cdot-}$ (0-20 μM). Inset: A linear correlation between the fluorescence intensity and $O_2^{\cdot-}$ concentrations. (b) One-photon fluorescence spectra of 10 μM TCA after adding 20 μM $O_2^{\cdot-}$ which was generated by Xanthine Oxidase. All of the spectra were acquired in 0.03 M Tris buffer (pH 7.4) at λ_{ex} = 491 nm.

5. The reversibility of TCA

The proposed reaction mechanism of TCA with $O_2^{\cdot-}$ was shown in Figure S3. We consider that the molar ratio between TCA and $O_2^{\cdot-}$ should be 1:2 from the study of the proposed reaction mechanism.

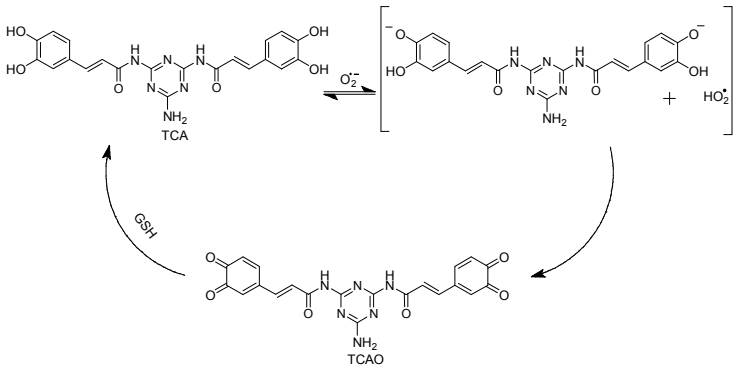

Figure S3 the proposed reaction mechanism

The reversibility of the probe was tested (Figure S4). This reversible cycle can be repeated for three times more under the same conditions. The reversibility implied the advantage of TCA for dynamic determine $O_2^{\cdot-}$ in cells and in vivo.

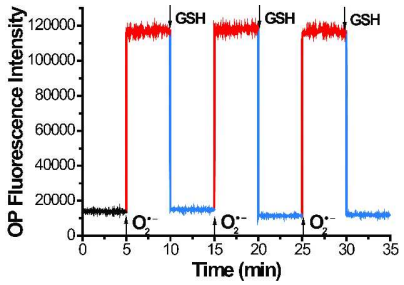

Figure S4 The reversibility of TCA. TCA was added with 20 μM $O_2^{\cdot-}$, after 5 min, the solution was treated with 2.0 mM GSH. When the fluorescence returned to the baseline level, another 20 μM $O_2^{\cdot-}$ was added to the mixture after 5 min. The cycles were repeated three times. All of the one-photon spectra were acquired in 0.03 M Tris buffer (pH 7.4) at λ_{ex} = 491 nm.

The fluorescence responses of TCAO to different concentrations of GSH were showed in Figure S5. The fluorescence of TCAO decreases gradually with the increase of GSH concentrations, until [GSH] reaches 2.0 mM. So 2.0 mM GSH was used to convert TCAO into TCA in the reversible cycle experiment. Moreover, the results showed TCAO instantaneously reacts with GSH, just as the instantaneous reaction between TCA and $O_2^{\cdot-}$.

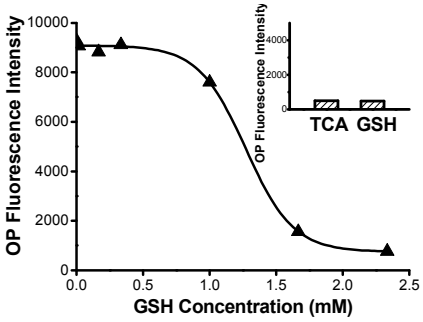

Figure S5 Fluorescence responses after adding various concentrations of GSH (0-2.3 mM) to reaction system (20 μM $O_2^{\cdot-}$ and 10 μM TCA). The one-photon fluorescent intensity was acquired in 0.03 M Tris buffer (pH 7.4), with excitation wavelength at 491 nm. Insert: TCA was insensitivity to GSH. The fluorescence of TCA was invariant upon the addition of GSH (3.0 mM).

6. The selectivity of TCA

The selectivity of TCA was studied. Figure S6 showed TCA was unperturbed upon the addition of various concentrations of reactive species. And Figure S7 revealed negligible fluorescence responses of TCA toward various concentrations of metal ions including Fe^{3+}, Fe^{2+}, Cu^{2+}, Cu^{+} and Zn^{2+}, even when Fe^{2+} coexists with H_2O_2 in order to generate •OH.

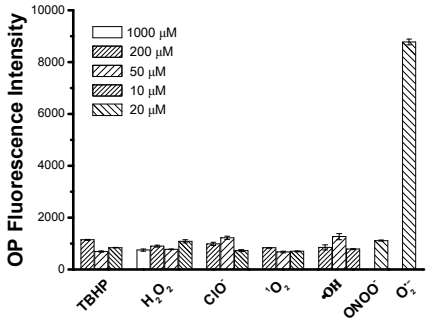

Figure S6 Fluorescence responses of 10 μM TCA to various reactive oxygen and nitrogen species. Bars represent the fluorescence after the addition of different concentration of each reactive species. Data were acquired in 0.03 M Tris, pH 7.4, with λ_{ex} = 491 nm.

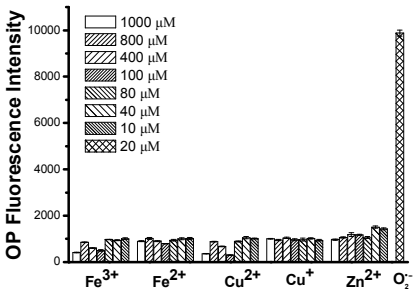

Figure S7 Fluorescence responses of 10 μM TCA to various metal ions. Bars represent the fluorescence after the addition of different concentration of metal ions. Data were acquired in 0.03 M Tris, pH 7.4, with λ_{ex} = 491 nm.

7. The instantaneous response and pH insensitivity

As showed in Figure S8 and S9, TCA displayed rapid response, good photostability, and pH insensitivity.

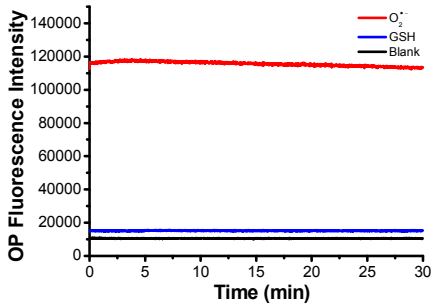

Figure S8 One-photon fluorescence response with time. Black line: 10 μM TCA. Red line: reaction system with 10 μM TCA and 20 μM $O_2^{\cdot-}$. Blue line: adding 2 mM GSH to the reaction system. Data were acquired in 0.03 M Tris, pH 7.4, with λ_{ex} = 491 nm.

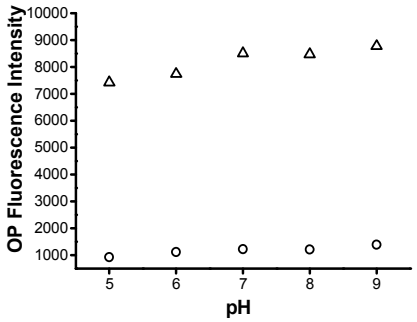

Figure S9 The one-photon fluorescent intensity of TCA (○) and reaction system with 20 μM $O_2^{\cdot-}$ (△) changed slightly in physiological pH range with excitation wavelength at 491 nm.

8. Cytotoxicity assay

HL-7702 cells (10^5 cell mL^{-1}) were dispersed within replicate 96-well microtiter plates to a total volume of 200 μL $well^{-1}$. Plates were maintained at 37 °C in a 5% CO_2/95% air incubator for 12 h. The cells were incubated for an additional 12 h with different concentrations probe (1×10^{-4}, 1×10^{-5} and 1×10^{-6}, 1×10^{-7} M). Subsequently, MTT (3-(4, 5-dimethylthiazol-2-yl) 2, 5-diphenyl tetrazolium bromide) solution (5 mg mL^{-1}, PBS) was then added to each well. After 4 h, the remaining MTT solution was removed, and 150 μL of DMSO was added into each well, followed by further incubation for 4 h at 37 °C. Absorbance was measured at 490 nm in a TRITURUS microplate reader. Calculation of IC50 value was done according to Huber and Koella[7]. Figure S10 showed that TCA was low toxic to cells over the course of imaging experiments.

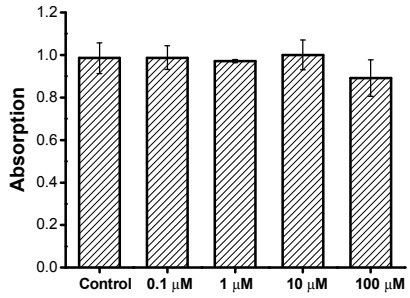

Figure S10 Viability of HL-7702 cells in the presence of TCA as measured by using MTT assay. The cells were incubated with TCA for 12 h. IC50 value was 0.7 mM.

9. Scavenger experiments in cell extracts

Fluorescence responses of TCA were studied using SOD and Tiron as $O_2^{\cdot-}$ scavengers in cellular extracts. The experiments summarized in Figure S11 showed that TCA fluoresced strongly in cell extracts stimulated with PMA. Upon the treatment of SOD or Tiron, TCA showed apparently lower fluorescence in the cell extracts upon PMA stimulation. These results established the scavenger capability using SOD and Tiron were identical.

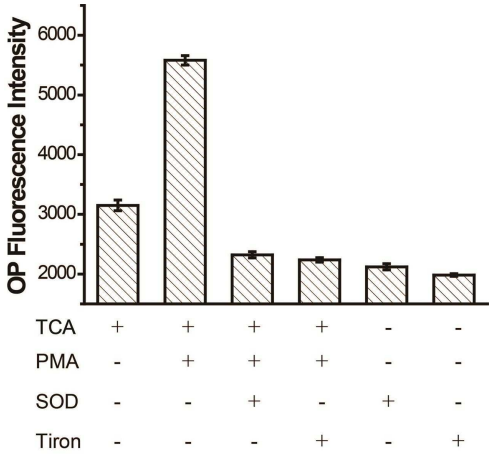

Figure S11 The fluorescent changes of scavenger experiments in cell extracts.

10. The main source of $O_2^{\cdot-}$ during hepatocytes reperfusion injury

In light of previous data, xanthine oxidase, the mitochondrial electron transport chain (complex I, II and III) and cyclooxygenase are thought to be enzymatic generating pathways of $O_2^{\cdot-}$ in hepatocytes.[8, 9] However, during hepatocytes reperfusion injury, the main source of $O_2^{\cdot-}$ is still uncertain. To solve this problem, five corresponding enzyme inhibitors[10-17] were selected to regulate $O_2^{\cdot-}$ levels, which was generated by the enzymes mentioned above (Figure S12). The OP imaging investigations showed that fluorescent intensity of hepatocytes decreased significantly in the presence of malonic acid (MA), which inhibited $O_2^{\cdot-}$ production from the mitochondrial respiratory chain complex II during OGD reperfusion. From the results, we speculated that mitochondrial respiratory chain complex II was the main source of the over-producing $O_2^{\cdot-}$ in hepatocytes under OGD reperfusion. Meanwhile, to further verify the major source of $O_2^{\cdot-}$ is mitochondrial respiratory chain complex II, we performed MTT cytotoxicity assay and obtained a consistent result with the hepatocytes OP images (Figure S13).

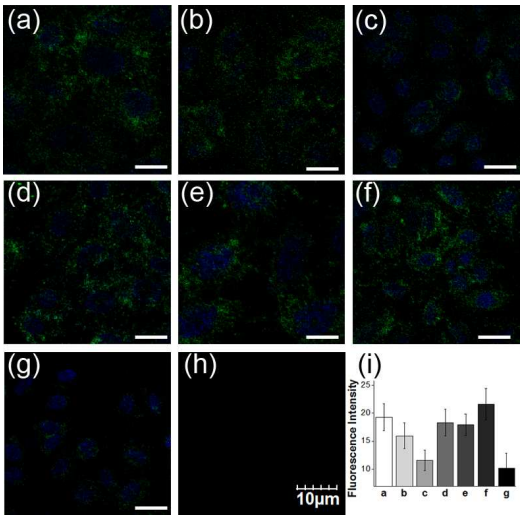

Figure S12 The influences of different inhibitors for superoxide generation under OGD (1% O_2 and glucose-free DMEM exposure) and reperfusion were visualized using the fluorescent probe TCA and confocal laser scanning microscopy. HL-7702 cells were pretreated with (a) 100 purinol, (b) 10 μM rotenone, (c) 100 μM malonic acid, (d) 100 μM 2,3-Dimercaptopropanol, (e) 200 μM Arcoxia, (f) no inhibitor and (g) all the five inhibitors. (i) Relative OP fluorescent intensity of TCA-labeled hepatic cells (a-g). (h) TP fluorescent images of HL-7702 cells were pretreated with 100 μM malonic acid under OGD reperfusion. The blue fluorescence was generated from Hoechst 33342 (10 μM). Images were acquired using 405 nm and 488 nm for OP excitation, and 770 nm for TP excitation, respectively. OP fluorescent emission windows: blue = 400−470 nm, green = 500−600 nm, and TP fluorescent emission windows: 500-550 nm. Scale bar = 15 μm. Cells shown are representative images from replicate experiments (n = 5).

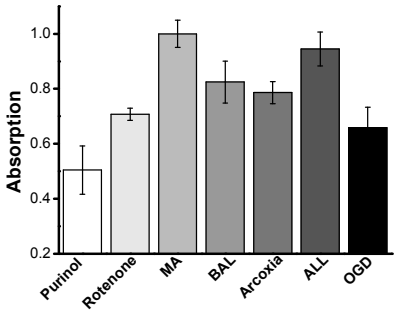

Figure S13 Viability of HL-7702 cells in the presence of inhibitors as measured by using MTT assay. These inhibitors are including purinol, rotenone, malonic acid (MA), 2, 3-Dimercaptopropanol (BAL) and Arcoxia. The cells were incubated under oxygen-glucose deprivation and reperfusion condition with each inhibitor, all the five inhibitors (All), or no (OGD) inhibitor for 0.5 h.

11 Dynamic imaging of $O_2^{\cdot-}$

The real-time changes of $O_2^{\cdot-}$ levels in PMA-stimulated HL-7702 cells were monitored. A noticeably fluorescence of TCA enhancement was observed during 20 minutes. It means that $O_2^{\cdot-}$ levels in

PMA-stimulated cells were gradually increased. The experiments indicated that TCA was capable to dynamically visualize intracellular $O_2^{\cdot-}$ levels.

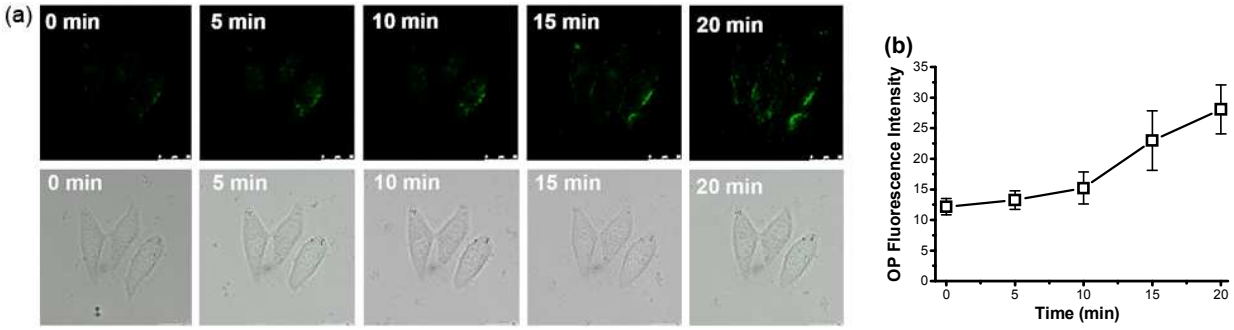

Figure S14 Real-time fluorescent imaging during PMA stimulation. (a) 10 μM TCA-loaded HL-7702 cells were treated with 5 mM 10 μg/mL PMA (0, 5, 10, 15 and 20 min). (b) Relative OP fluorescent intensity of TCA-labeled cells in fig a. Cells shown are representative images from replicate experiments (n = 5). Scale bar = 15 μm.

12. Imaging of zebrafish

Interestingly, by means of OP imaging, we found that $O_2^{\cdot-}$ largely distributed in liver and heart of zebrafish after oxygen deprivation reperfusion. Meanwhile we observed that the $O_2^{\cdot-}$ concentrations gradually increased with time prolonging (Fig. S15a). At depth of 180 μm inside zebrafish, we captured clearer TP imaging of $O_2^{\cdot-}$ distribution profile (Fig. S15b).

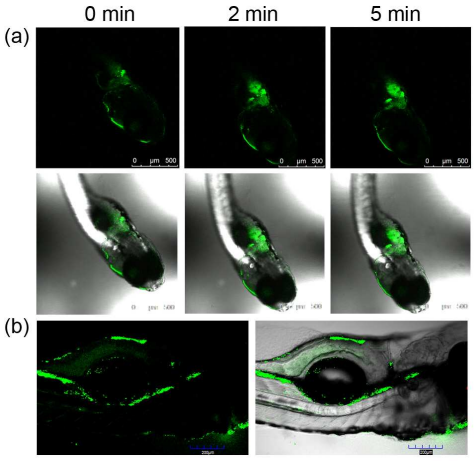

Figure S15 Fluorescent images of $O_2^{\cdot-}$ levels in zebrafish before and after reperfusion. (a) OP fluorescent images of zebrafish and the overlay of darkfield and brightfield after reperfused were captured in 0, 2, and 5 min. The zebrafish was pretreated with TCA and sodium hydrosulfite in water for 15 min, and then was reperfused with dissolving oxygen water. (b) TP fluorescent images and the overlay of darkfield and brightfield of zebrafish after reperfusion. Images were acquired using 488 nm (OP) and 770 nm (TP) excitation respectively. OP fluorescent emission windows: green= 500−600 nm, and TP fluorescent emission windows: 500-550 nm Scale bar, 500 μm.

13. Cell, zebrafish and mice culture

A human hepatic cell line (HL-7702) and HepG2 cells were cultured in high glucose DMEM (4.5 g of glucose/L) supplemented with 10% fetal bovine serum, 1% penicillin, and 1% streptomycin at 37 ℃ (w/v) in a 5% CO_2/95% air incubator MCO-15AC (SANYO, Tokyo, Japan). One day before imaging, the cells were detached and were replanted on glass-bottomed dishes.

The concentration of counted cells for cell extracts was 1×10^6 cells mL^{-1}. Parts of normal cultured or PMA-stimulated cells were incubated with TCA for 30 min and washed twice with Tris-HCl buffer. All the cells were suspended in a volume of Tris and disrupted for 10 min in a VC 130PB ultrasonic disintegrator (<4 ^oC). The broken cell suspension was centrifuged at 4000 rpm for 10 min and the pellet discarded. Cell extracts were divided into several parts, and added with SOD (200 U) or Tiron (10 μM).

Hepatic cells in the OGD group were cultured in DMEM without glucose containing a deoxygenated reagent 0.5 mmol/L sodium dithionite for 0.5 h[18]. After that, the cells were incubated again in DMEM containing glucose with 5% CO_2 and 95% O_2 for 0.5 h.

Wild type zebrafish was from Shandong Academy of Sciences. Seven days post fertilization zebrafish was incubated in 10 μM probe for 0.5 h and then imaged using confocal fluorescence microscopy. The zebrafish in treatment were placed in confocal culture dish.

Eight- to ten-week-old wild-type BalB/C mice (male) were used. The mice were anesthetized with 4% chloral hydrate (3 mL/kg) by intraperitoneal injection and a laparotomy was performed to expose the liver[19]. Hepatic ischemia was induced by clamping the artery to the left lobe of the liver. Thirty minutes later, the ischemic liver was reperfused by opening the vascular clamp. Then TCA (100 μM) was adding in the left lobe of the liver. As a control, the mice were exposed the liver and added TCA (100 μM) in the left lobe of the liver. The mice were then imaged (30 min after the injection of TCA) by using a Leica TCS MP5 in vivo imaging system.

14. Confocal imaging and two-photon fluorescence imaging

One-photon fluorescent images were acquired on a Leica TCS SP5 confocal laser-scanning microscope with an objective lens (×40). The excitation wavelength was 405 nm (5 mW), and 488 nm (15

mW) respectively. Following incubation, the cells were washed three times with DMEM without FBS and imaged.

The TP imaging of cells and zebrafish were obtained with Olympus FV1000MPE with a 60× water objective and the TP imaging of mice were obtained with Leica TCS MP5 with a 25× water objective. All the Ti:sapphire laser was used to excite the specimen at 770 nm and transmissivity was 6%.

15. Measurement of two-photon cross section

The two-photon cross section (δ) was determined by using femto second (fs) fluorescence measurement technique[20]. TCAO were dissolved in 30 mM Tris buffer at the concentration of 1.0×10^{-5} M and then the two-photon induced fluorescence intensity was measured at 800 nm by using fluorescein (1.0×10^{-5} M, pH 11) as the reference, whose two-photon property has been well characterized in the literature. The intensities of the two-photon induced fluorescence spectra of the reference and sample emitted at the same excitation wavelength were determined. The TPA cross section was calculated according to Eq (1).

$$\delta_s = \delta_r \frac{\Phi_r}{\Phi_s} \frac{C_r}{C_s} \frac{n_r}{n_s} \frac{F_s}{F_r} \qquad (1)$$

The subscripts s and r refer to the sample and the reference material, respectively. δ is the TPA cross sectional value, C is the concentration of the solution, n is there refractive index of the solution, F is two-photon excited fluorescence integral intensity and Φ is the fluorescence quantum yield. Here the fluorescence quantum yield of TCAO is 0.135 (Tris buffer) using fluorescein as the reference[21].

The result shows that the two-photon cross section of TCAO in Tris buffer at pH 7.4 is 22 GM.

Reference

(1) Carpenter, J. E.; Weinhold, F. *J. Mol. Struc. Theochem.* **1988,** *46*, 41-62.
(2) Reed, A. E.; Weinhold, F. *J. Chem. Phys.* **1983,** *78*, 4066-4073.
(3) Foster, J. P.; Weinhold, F. *J. Am. Chem. Soc.* **1980,** *102*, 7211-7218.
(4) Glendening, E. D.; Reed, A. E.; Carpenter, J. E.; Weinhold, F. NBO Version 3.1.
(5) Frisch, M. J.; Trucks, G. W.; Schlegel, H. B.; Scuseria, G. E.; Robb, M. A.; Cheeseman, J. R.; Montgomery, J. A.; Vreven, T. Jr.; Kudin, K. N.; Burant, J. C.; Millam, J. M.; Iyengar, S. S.; Tomasi, J.; Barone, V.; Mennucci, B.; Cossi, M.; Scalmani, G.; Rega, N.; Petersson, G. A.; Nakatsuji, H.; Hada, M.; Ehara, M.; Toyota, K.; Fukuda, R.; Hasegawa, J.; Ishida, M.; Nakajima, T.; Honda, Y.; Kitao, O.; Nakai, H.; Klene, M.; Li, X.; Knox, J. E.; Hratchian, H. P.; Cross, J. B.; Bakken, V.; Adamo, C.; Jaramillo, J.; Gomperts, R.; Stratmann, R. E.; Yazyev, O.; Austin, A. J.; Cammi, R.; Pomelli, C.; Ochterski, J. W.; Ayala, P. Y.; Morokuma, K.; Voth, G. A.; Salvador, P.; Dannenberg, J. J.; Zakrzewski, V. G.; Dapprich, S.; Daniels, A. D.; Strain, M. C.; Farkas, O.; Malick, D. K.; Rabuck, A. D.; Raghavachari, K.; Foresman, J. B.; Ortiz, J. V.; Cui, Q.; Baboul, A. G.; Clifford, S.; Cioslowski, J.; Stefanov, B. B.; Liu, G.; Liashenko, A.; Piskorz, P.; Komaromi, I.; Martin, R.

L.; Fox, D. J.; Keith, T.; Al-Laham, M. A.; Peng, C. Y.; Nanayakkara, A.; Challacombe, M.; Gill, P. M. W.; Johnson, B.; Chen, W.; Wong, M. W.; Gonzalez, C.; Pople, J. A. Gaussian03, revision B.04; Gaussian, Inc, Wallingford, CT, **2004**.
(6) Hay, P. J.; Wadt, W. R. J. *Chem. Phys.* **1985**, *82*, 270-299.
(7) Huber, W.; Koella, *J. C. Acta Trop*. **1993**, *55*, 257-261.
(8) Love, S. *Brain. Pathol.* **1999**, *9*, 119-131.
(9) Turrens, J. F. *J. Physiol.* **2003**, *552*, 335-344.
(10) Mayes, P. A.; Botham, K. M. The respiratory chain & oxidative phosphorylation. Harper's Biochemistry. 23rd ed. East Norwalk, Connecticut: Appleton and Lange, Prentice-Hall International, Inc, **1993**, 119-130.
(11) Liu, J.; Cao, L.; Chen, J.; Song, S.; Lee, I. H.; Quijano, C.; Liu, H.; Keyvanfar, K.; Chen, H.; Cao, L. Y; Ahn, B. H; Kumar, N. G.; Rovira, I. I.; Xu, X. L; Lohuizen, M.; Motoyama, N.; Deng, C. X; Finkel, T. *Nature* **2009**, *459*, 387-392.
(12) Muller, F.; Liu, Y.; Abdul-Ghani, M.; Lustgarten, M., Bhattacharya, A.; Jang, Y.; Van Remmen, H. *Biochem. J.* **2008**, *409*, 491-499.
(13) Dannhardt, G.: Kiefer, W. *Eur. J. Med. Chem.* **2001**, *36*, 109-126.
(14) Riendeau, D.; Percival, M. D.; Brideau, C.; Charleson, S.; Dube, D.; Ethier, D.; Falgueyret, J. P.; Friesen, R. W.; Gordon, R.; Greig, G.; Guay, J.; Mancini, J.; Ouellet, M.; Wong, E.; Xu, L.; Boyce, S.; Visco, D.; Girard, Y.; Prasit, P.; Zamboni, R.; Rodger, I. W.; Gresser, M.; Ford-Hutchinson, A. W.; Young, R. N.; Chan, C. C. *J. Pharmacol. Exp. Ther.* **2001**, *296*, 558-566.
(15) Linas, S. L.; Whittenburg, D.; Repine, J. E. *Am. J. Physiol. Renal. Physiol.* **1990**, *258*, F711-F716.
(16) Wojtovich, A. P.; Brookes, P. S. *Biochim Biophys Acta.* **2008**, *1777*, 882-889.
(17) Liu, Y.; Fiskum, G.; Schubert, D. *J. Neurochem.* **2002**, *80*, 780-787.
(18) Liu, R.; Zhang, L.; Lan, X.; Li, L.; Zhang, T. T.; Sun, J. H.; Du, G. H. *Neuroscience* **2011**, *176*, 408-419.
(19) Thiberge, S.; Blazquez, S.; Baldacci, P.; Renaud, O.; Shorte, S.; Ménard, R.; Amino, R. *Nat. Protoc.* **2007**, *2*, 1811-1818.
(20) Xu, C.; Webb, W. W. *J. Opt. Soc. Am. B*. **1996**, *13*, 481–491.
(21) Lakowicz, J. R. Principles of Fluorescence Spectroscopy, 2nd Ed. Kluwer Academic/Plenum Publishers, New York, London, Moscow, Dordrecht, **1999**.